Soluble epoxide hydrolase regulates hematopoietic progenitor cell function via generation of fatty acid diols

Timo Frömel[a], Benno Jungblut[b], Jiong Hu[a], Caroline Trouvain[a], Eduardo Barbosa-Sicard[a], Rüdiger Popp[a], Stefan Liebner[c], Stefanie Dimmeler[d], Bruce D. Hammock[e,1], and Ingrid Fleming[a,1]

[a]Institute for Vascular Signalling, [c]Institute of Neurology, and [d]Institute for Cardiovascular Regeneration, Goethe University, Frankfurt am Main D-60596, Germany; [b]Department of Cardiac Development and Remodeling, Max Planck Institute for Heart and Lung Research, 61231 Bad Nauheim, Germany; and [e]Department of Entomology and Cancer Center, University of California, Davis, CA 95616

Contributed by Bruce D. Hammock, April 28, 2012 (sent for review November 20, 2011)

Fatty acid epoxides are important lipid signaling molecules involved in the regulation of vascular tone and homeostasis. Tissue and plasma levels of these mediators are determined by the activity of cytochrome P450 epoxygenases and the soluble epoxide hydrolase (sEH), and targeting the latter is an effective way of manipulating epoxide levels in vivo. We investigated the role of the sEH in regulating the mobilization and proliferation of progenitor cells with vasculogenic/reparative potential. Our studies revealed that sEH down-regulation/inhibition impaired the development of the caudal vein plexus in zebrafish, and decreased the numbers of lmo2/cmyb-positive progenitor cells therein. In mice sEH inactivation attenuated progenitor cell proliferation (spleen colony formation), but the sEH products 12,13-dihydroxyoctadecenoic acid (12,13-DiHOME) and 11,12- dihydroxyeicosatrienoic acid stimulated canonical Wnt signaling and rescued the effects of sEH inhibition. In murine bone marrow, the epoxide/diol content increased during G-CSF–induced progenitor cell expansion and mobilization, and both mobilization and spleen colony formation were reduced in sEH$^{-/-}$ mice. Similarly, sEH$^{-/-}$ mice showed impaired functional recovery following hindlimb ischemia, which was rescued following either the restoration of bone marrow sEH activity or treatment with 12,13-DiHOME. Thus, sEH activity is required for optimal progenitor cell proliferation, whereas long-term sEH inhibition is detrimental to progenitor cell proliferation, mobilization, and vascular repair.

beta-catenin | ischemic hindlimb | linoleic acid

Cytochrome P450 (CYP) enzymes are involved in numerous detoxification and synthetic processes in addition to generating potent lipid mediators from endogenous substrates. Even though many CYP isozymes can oxidize a spectrum of n-6 and n-3 polyunsaturated fatty acids (PUFA), such as retinoic acid, linoleic acid, eicosapentaenoic acid, and docosahexenoic acid, they are often referred to as the third pathway of arachidonic acid metabolism, mainly because most is known about the biological actions of these products (1).

Since the first report that CYP-derived metabolites of arachidonic acid can elicit vascular smooth-muscle hyperpolarization and relaxation (2, 3), it has become clear that the arachidonic acid epoxides or epoxyeicosatrienoic acids (EETs) are important lipid signaling molecules implicated in vascular remodeling and the attenuation of inflammation (4). A role for CYP enzymes in angiogenesis has been repeatedly demonstrated in different in vitro models, as have corresponding effects on vascular development in EET-impregnated Matrigel plugs in mice and in the chick chorioallantoic membrane (for review, see ref. 5). However, many such studies were performed in overexpressing systems, and there are difficulties in backing up these findings in knockout models because major differences in CYP epoxygenase isoform expression exist between humans and rodents. This finding is particularly true for the CYP2C family of proteins, which have been most frequently linked to angiogenesis (5) and which are able to oxidize arachidonic acid as well as many other PUFAs. Furthermore, zebrafish, a useful model for studying vascular development, express 47 isoforms of the CYP2 genes compared with 16 in humans (6). An alternative to modulating epoxide production is to prevent their metabolism by inhibiting the soluble epoxide hydrolase (sEH). The latter enzyme metabolizes the PUFA epoxides to their corresponding diols [e.g., EETs to dihydroxyeicosatrienoic acids (DHETs)] and is highly conserved between species. Therefore, the aim of the present study was to investigate the consequences of interfering with sEH activity and expression on vascular development and vascular repair processes.

Results

sEH Knockdown in Zebrafish Causes Defects in the Caudal Vein Plexus. Zebrafish expressed a protein (Ensembl gene ID:ENSDARG00000040255) with ~60% identity to the hydrolase domain of the human sEH. Protein sequence alignment of the hydrolase domain with other vertebrate species revealed a high level of homology in the residues that form the catalytic triad, as well as the tyrosine residues that are assumed to be important for the positioning of the substrate (7). The protein was recognized by antibodies raised against the rat sEH and, when overexpressed in Sf9 cells, the zebrafish protein generated 14,15-DHET from 14,15-EET and was sensitive to sEH but not microsomal EH inhibitors (Fig. S1).

Blocking the translation (ATG morpholino) or the correct splicing of the sEH (morpholinos directed against exon 13 or exon 17) in zebrafish embryos almost abrogated sEH protein expression and activity (Fig. 1*A*). In transgenic *kdrl:EGFP* zebrafish embryos in which the developing vasculature/endothelial cells are labeled green, sEH down-regulation induced only minor changes in the arterial vasculature of the embryo trunk, because the primary vessel, intersegmental vessels, and the dorsal anastomotic vessels all appeared normal. However, parachordal vessels were consistently (10 of 10 morphants) either disorganized/misguided (Fig. 1*B*, arrows) or missing completely (Fig. 1*B*, arrowheads). sEH down-regulation, however, did consistently result in smaller eyes and the remodeling of the caudal vein plexus (CVP) into a single venous vessel in 32 of 32 sEH ATG and exon 13 morphants (Fig. 1*B* and Fig. S2*A*).

Author contributions: T.F., B.J., and I.F. designed research; T.F., B.J., J.H., C.T., E.B.-S., and R.P. performed research; S.L., S.D., and B.D.H. contributed new reagents/analytic tools; T.F., B.J., J.H., C.T., E.B.-S., R.P., S.D., and I.F. analyzed data; and T.F., B.D.H., and I.F. wrote the paper.

The authors declare no conflict of interest.

[1]To whom correspondence may be addressed. E-mail: bdhammock@ucdavis.edu or fleming@em.uni-frankfurt.de.

This article contains supporting information online at www.pnas.org/lookup/suppl/doi:10.1073/pnas.1206493109/-/DCSupplemental.

MEDICAL SCIENCES

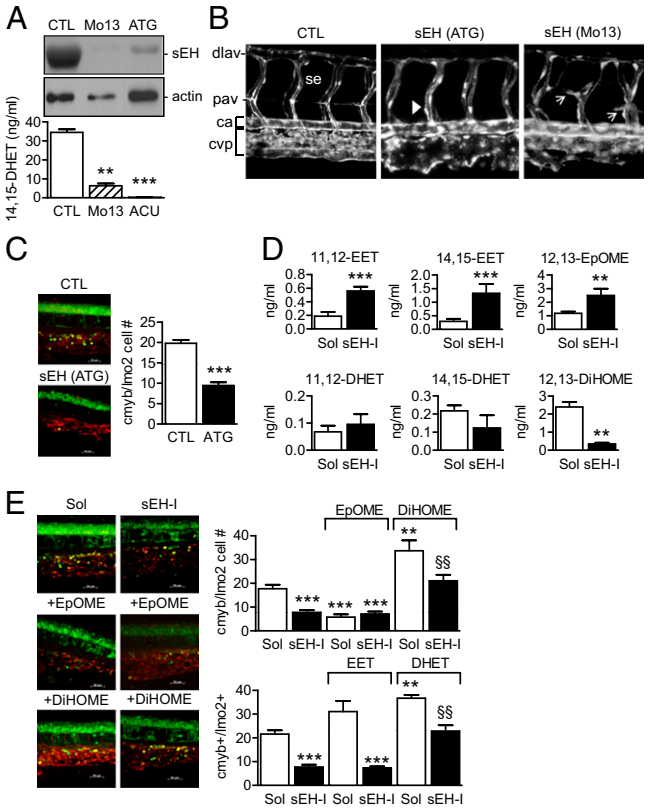

Fig. 1. Role of the sEH in the differentiation of the CVP and the caudal hematopoietic tissue in zebrafish. (*A*) sEH protein expression and activity in 4-d-old zebrafish embryos treated with control (CTL), sEH-ATG or sEH-Mo13 morpholinos. (*B*) Confocal images of the CVP in *Tg(kdrl:EGFP)* zebrafish (48 hpf) treated with control or sEH morpholinos. The anterior part of the embryos is on the left; ca, caudal artery; dlav, dorsal longitudinal anastomotic vessel; se, intersegmental vessel; pav, parachordal vessel. Arrows indicate the delayed secondary sprouting of the parachordal vessels, whereas arrowheads mark missing vessels. (*C*) Effect of control versus sEH (ATG) morpholinos on the number of *cmyb*$^+$GFP/*lmo2*$^+$dsRED cells in the CVP in a 40× field *z*-stack projection located posterior of the yolk sac extension. (*D*) 11,12-, 14,15-EET/DHET and 12,13-EpOME/DiHOME levels in extracts from 4-d-old zebrafish treated with solvent (Sol) or the sEH inhibitor *t*-AUCB (sEH-I). (*E*) Effect of *t*-ACUB, 12,13-EpOME, or 12,13-DiHOME on the number of *cmyb*$^+$GFP/*lmo2*$^+$dsRED cells in the CVP (four-somite stage until 36 hpf). The graphs summarize data obtained with 5–17 zebrafish per group; $^{**}P < 0.01$, $^{***}P < 0.001$ vs. Sol or CTL, $^{\S\S}P < 0.01$ vs. sEH-I alone. (Magnification: *B*, 100×; *E*, 400×.)

The CVP is a complex vessel network that originates from the single channeled caudal vein 24–48 hours postfertilization (hpf) and serves as a transient hematopoietic tissue where hematopoiesis and angiogenesis occur in a close physical proximity (8). We therefore studied a subpopulation of hematopoietic cells in bigenic *cmyb:GFP/lmo2:DsRed* zebrafish embryos (i.e., green-labeled hematopoietic stem cells and progenitors; red-labeled hematopoietic stem cells and endothelium) (9). Fewer *cmyb/lmo2* double-positive cells were detected within the CVP in sEH (ATG) morphants than in the zebrafish injected with a control morpholino 36 hpf (Fig. 1*C*) and 55 hpf (Fig. S3*A*). Similar results were obtained using morpholinos directed against exon 17. In addition, histone 3 phosphorylation in cmyb:GFP cells was significantly ($64 \pm 16\%$, $P < 0.05$, $n = 7$) attenuated by sEH knockdown. We also detected fewer CD41:GFP cells [i.e., definitive hematopoietic stem cells in morpholino (ATG)-treated zebrafish after 55 and 72 hpf] (Fig. S3*B*).

The sEH was named on the basis of its ability to metabolize epoxides but the enzyme possesses two functional domains: a C-terminal epoxide hydrolase and an N-terminal lipid phosphatase (10, 11). To ensure that the defects observed could be attributed to the loss of epoxide hydrolase activity, we assessed the consequences of treating embryos with the sEH inhibitor, *trans*-4-[4-(3-adamantan-1-ylureido)cyclohexyloxy]-benzoic acid (*t*-AUCB) (12). A similar caudal vein phenotype (including the formation of a single venous vessel) was detected in sEH inhibitor-treated embryos but there was no effect of the sEH inhibitor on the size of the zebrafish eye (Fig. S4). The next step was to analyze the epoxides/diols generated by zebrafish treated with solvent or *t*-AUCB (Fig. S5). Of the epoxide/diol pairs studied, the most pronounced sEH inhibitor-related changes were observed for the arachidonic acid-derived 11,12-EET/DHET and 14,15-EET/DHET, and the linoleic acid-derived 12,13-epoxyoctadecenoic acid (12,13-EpOME)/12,13-dihydroxyoctadecenoic acid (12,13-DiHOME) (Fig. 1*D*). To determine which of the lipid mediators contributes to the recruitment of *cmyb/lmo2* double-positive cells to the CVP, we performed rescue experiments by administering the epoxides and diols to embryos treated with the sEH inhibitor which, similar to the morpholino-mediated down-regulation of the sEH, also decreased numbers of *cmyb/lmo2* double-positive cells within the CVP 36 hpf (Fig. 1*E*). We found that although 11,12-EET increased the numbers of *cmyb/lmo2* double-positive cells in solvent-treated zebrafish embryos, it was unable to rescue the effect of the sEH inhibitor (Fig. 1*E*). On the other hand, 11,12-DHET increased *cmyb/lmo2* double-positive cells in embryos treated with *t*-AUCB to levels seen in solvent treated embryos. 14,15-EET and 14,15-DHET were without effect. Interestingly, 12,13-EpOME was just as effective as the sEH inhibitor in attenuating *cmyb/lmo2* cell numbers, and 12,13-DiHOME reversed the effects of sEH inhibition (Fig. 1*E*). Because the 12,13-EpOME/DiHOME levels in zebrafish were consistently higher than those of 11,12-EET/DHET and the EpOME decreased as DiHOME increased cell numbers, these data indicated that the epoxides and diols of linoleic acid potentially make a greater contribution to the phenotype observed.

sEH Inhibition Decreases Bone Marrow Cell Colony Formation. We next determined whether the effects observed in zebrafish could be applicable to progenitor cell expansion and differentiation in mammals. Murine bone marrow contained sEH protein (Fig. 2*A*) and bone marrow-derived hematopoietic progenitor cells (HPC) [i.e., lineage-negative (Lin$^-$) cKit-positive (cKit$^+$) cells], showed robust sEH activity (Fig. 2*B*). Bone marrow cells also generated 9,10- and 11,12-EpOME/DiHOME, as well as 11,12- and 14,15-EET/DHET. As with the zebrafish, levels of the EpOMEs/DiHOMEs were higher than those of the EETs/DHETs (Fig. 2*C*). To parallel the studies in zebrafish, we assessed the ability of the sEH to influence the formation of short-term repopulating HPC colonies in spleens from irradiated WT animals (CFU-S12 assay). Solvent-treated bone marrow cells from sEH$^{-/-}$ mice formed significantly fewer colonies than cells from WT mice (Fig. 2*D*), an effect reproduced by pretreating WT cells with the sEH inhibitor, *t*-AUCB, before transplantation (Fig. 2*G*). Incubation of WT bone marrow cells with 11,12-EET, 11,12-DHET, 12,13-EpOME, or 12,13-DiHOME before transplantation increased subsequent colony formation. However, only 11,12-DHET and 12,13-DiHOME increased the ability of cells from sEH$^{-/-}$ mice to form colonies, with the latter being more effective. Similar results were obtained when BrdU incorporation and histone 3 phosphorylation were assessed as indices of HPC proliferation (Fig. S6). As cells from WT mice were able to generate diols from the exogenously applied epoxides, these data suggested that the lack of diol production rather than accumulation of epoxide was responsible for the effects observed in sEH$^{-/-}$ mice.

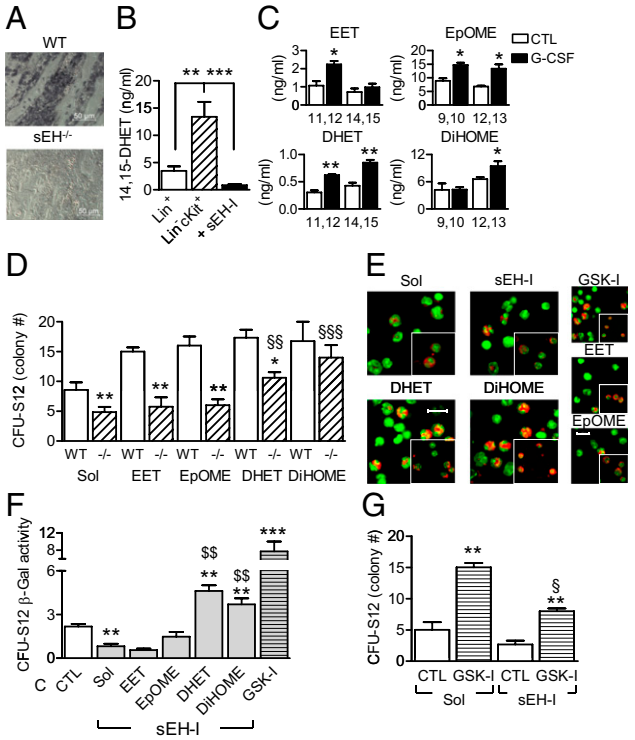

Fig. 2. Effect of EET/DHET and EpOME/DiHOME on HPCs and β-catenin activation in mice. (*A*) sEH expression in the murine femur (alkaline phosphatase). (*B*) sEH activity (LC-MS/MS) in Lin$^+$ and Lin$^-$cKit$^+$ cells in the absence and presence of the sEH inhibitor *t*-AUCB (sEH-I). (*C*) Comparison of bone marrow cell EET/DHET and EpOME/DiHOME levels in WT mice following treatment with saline (CTL) or G-CSF (3 d). (*D*) Ability of bone marrow cells from WT and sEH$^{-/-}$ mice to form colonies in the spleens of irradiated WT mice. Cells were treated with either solvent (Sol), 11,12-EET/DHET or 12,13-EpOME/DiHOME for 4 h before transplantation and spleen colony formation was assessed after 12 d. (*E*) Effect of solvent, the sEH inhibitor *t*-AUCB (sEH-I), the GSK inhibitor (GSK-I) 6-bromoindirubin-3′-oxime, 11,12-EET/DHET, and 12,13-EpOME/DiHOME on β-catenin levels (red) in bone marrow cells from WT mice. (*Insets*) β-Catenin levels in Lin$^-$ cells; green, DAPI. (Scale bar, 10 μm.) (*F*) Effect of 11,12-EET/DHET and 12,13-EpOME/DiHOME on β-galactosidase activity in spleen cells isolated from irradiated mice 12 d after transplantation with bone marrow from TOP-Gal mice. (*G*) Spleen colony formation 12 d after transplantation of Lin$^-$ cells from WT mice treated ex vivo with either solvent, *t*-ACUB (sEH-I) alone or in combination with 11,12- EET/DHET and 12,13-EpOME/DiHOME, or GSK inhibitor (GSK-I) LiCl. The graphs summarize data obtained with four to seven animals per group; $^*P < 0.05$, $^{**}P < 0.01$, $^{***}P < 0.001$ vs. CTL, $^{\S\S}P < 0.01$, $^{\S\S\S}P < 0.001$ vs. Solvent-treated sEH$^{-/-}$ mice and \$\$ vs. the corresponding epoxide.

DiHOME and β-Catenin. Given that genetic deletion, as well as inhibition of the sEH, attenuated HPC proliferation—a process known to be linked to canonical Wnt signaling (13)—we determined whether the epoxides or diols studied could affect β-catenin activity. The 12,13-DiHOME and 11,12-DHET, but not 11,12-EET or 12,13-EpOME, were able to induce the nuclear translocation of β-catenin in Lin$^-$ bone marrow cells (Fig. 2*E*). When TOP-Gal mice, a reporter strain that express β-galactosidase in the presence of activated β-catenin (14), were used as donors for the CFU-S12 assay, we found that sEH inhibition attenuated β-galactosidase activity; DHET and DiHOME reversed this effect and the EET and EpOME were without effect (Fig. 2*F*). This link between the CYP/sEH axis and the Wnt signaling cascade was substantiated by the fact that the inhibition of GSK3 partly reversed the attenuated colony forming activity of sEH inhibitor-treated bone marrow cells (Fig. 2*G*).

We next determined whether or not the sEH affects mobilization in addition to proliferation. The activation of HPCs with G-CSF (2 d) resulted in altered bone marrow 11,12-EET/DHET, 14,15-DHET, as well as 9,10-EpOME and 12,13-EpOME/DiHOME levels (Fig. 2*C*), without affecting sEH expression. These changes in bone marrow lipid production were also reflected in plasma from WT but not sEH$^{-/-}$ mice after 5-d treatment with G-CSF when cell egress reached its maximum (Fig. S7). To link the latter phenomena to the HPC pool size in the bone marrow, peripheral blood mononuclear cells (PBMC) were collected after 5-d treatment with G-CSF and either quantified by colony generation in vitro (CFU-C assay), or transplanted into irradiated WT mice and colony formation monitored in the spleen over 12 d (CFU-S12 assay). A slight but nonsignificant decrease in CFU-C generation by cells from sEH$^{-/-}$ was apparent under basal conditions. The administration of G-CSF increased CFU-C formation by WT cells but significantly fewer colonies formed when cells were isolated from sEH$^{-/-}$ mice (Fig. 3*A*). Although significant differences were detected in the formation of granulocytes, erythrocytes, macrophages, and megakaryocytes (GEMM) and granulocytes and macrophages (GM) colonies, no difference could be detected in the G or M colonies (Fig. S8*A*). These findings fit well with the fact that fewer Lin$^-$Sca-1$^+$cKit$^+$ cells were recovered from the blood of sEH$^{-/-}$ than WT mice after 5-d G-CSF treatment (Fig. 3*B*). Moreover, in the CFU-S12

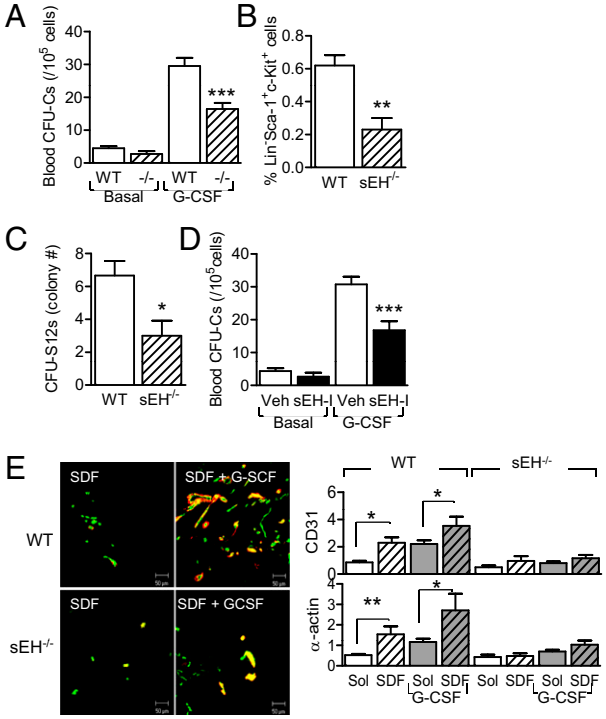

Fig. 3. Consequences of sEH deletion/inhibition on progenitor cell mobilization. (*A*) CFU-C colony formation by PBMCs from WT and sEH$^{-/-}$ mice under basal conditions and following treatment with G-CSF (5 d). (*B*) Percentage of Lin$^-$Sca-1$^+$c-Kit$^+$ cells derived from peripheral blood following treatment with G-CSF (5 d). (*C*) Spleen colony formation 12 d after transplantation of WT mice with PBMCs from G-CSF-treated WT or sEH$^{-/-}$ animals. (*D*) CFU-C colony formation by PBMCs from WT mice treated with vehicle (Veh) or the sEH inhibitor (sEH-I) *t*-AUCB under basal conditions and after treatment with G-CSF. (*E*) Cell invasion into Matrigel plugs impregnated with either solvent (PBS) or SDF-1. Animals were treated with either vehicle or G-CSF (5 d). Images were taken after sectioning and immunostaining of Matrigel plugs for CD31 (red) and α-actin (green) 9 d after implantation. The graphs summarize data obtained with 5–10 animals per group; $^*P < 0.05$, $^{**}P < 0.01$, $^{***}P < 0.001$.

MEDICAL SCIENCES

assay fewer colonies were formed in the spleens of sEH$^{-/-}$ mice (Fig. 3*C*). Similar observations were made when cells were recovered from spleens after 4-d treatment with saline or G-CSF and maintained in endothelial basal medium to generate cells previously referred to as "early endothelial progenitor cells" (Fig. S8*B*). sEH inhibition significantly increased circulating epoxide levels in WT mice (the EET/DHET ratio increased from 1.0 ± 0.3–2.1 ± 0.26 for 11,12-EET/DHET; $n = 4$, $P = 0.03$), and reproduced the phenotype recorded in the sEH$^{-/-}$ mice (i.e., resulted in the decreased mobilization of progenitor cells) (Fig. 3*D*).

Because Lin$^-$Sca-1$^+$cKit$^+$ cells give rise to neutrophils and monocytes, which contribute to angiogenesis and 11,12-EET increases the vascularization of acellular matrices, we compared the vascularization of Matrigel plugs in WT and sEH$^{-/-}$ mice. The matrix material was impregnated with solvent or the homing factor, stromal cell-derived factor-1 (SDF-1) and implanted into animals that were then treated with saline or G-CSF (5 d). After an additional 4 d the plugs were removed and endothelial cells (CD31) and pericytes/smooth-muscle cells (α-actin) in plugs were quantified. CD31 and α-actin–positive cells were detected in Matrigel plugs from WT animals treated with saline and vascularization increased when animals were treated with G-CSF. However, although the numbers of invading CD31- and α-actin–positive cells were comparable in both strains when treated with saline, the response to G-CSF was markedly diminished in sEH$^{-/-}$ mice (Fig. 3*E*).

To determine whether the defects observed in G-CSF–induced progenitor cell mobilization could be reproduced by a physiological stimulus such as hypoxia, the recovery of blood flow after hindlimb ischemia was compared in the WT and sEH$^{-/-}$ mice. Consistent with the attenuated mobilization of circulating progenitor cells, blood flow (Fig. 4*A*) and vascularization (Fig. 4*B*) in the ischemic limb recovered more slowly in sEH$^{-/-}$ than in WT animals. As EETs regulate blood flow in different tissues, it was conceivable that the consequences of sEH deletion/inhibition might be because of altered blood flow through the progenitor cell niche. To ensure that the effects observed could be attributed to a defect in progenitor cell function, we generated chimeric WT^{sEH} and sEH^{WT} mice in which bone marrow from sEH$^{-/-}$ mice was transplanted into WT mice and vice versa. This procedure restored sEH activity to bone marrow from sEH^{WT} mice (Fig. S9*A*) as well as the basal plasma epoxide/diol levels and G-CSF–induced changes when assessed 16 wk after transplantation (Fig. S9*B*). The attenuated recovery of colony-forming cells after G-CSF was maintained in sEH^{sEH} mice vs. WT^{WT} animals but mobilization of colony-forming cells was increased in sEH^{WT} mice and significantly decreased in WT^{sEH} mice (Fig. 4*C*). This procedure also partially reversed the phenotype of the animals and the extent of recovery from hindlimb ischemia, so that blood flow and vascularization in sEH^{WT} mice recovered more quickly than in WT^{sEH} animals (Fig. 4 *D* and *E*). To parallel the rescue experiments performed with the zebrafish, we determined the ability of EpOME vs. DiHOME to accelerate the recovery of blood flow in WT and sEH$^{-/-}$ mice. We found that the treatment of WT mice with 12,13-EpOME or 12,13-DiHOME failed to increase blood flow to the ischemic limb but 12,13-DiHOME—though not 12,13-EpOME—restored recovery in sEH$^{-/-}$ mice (Fig. 4*F*).

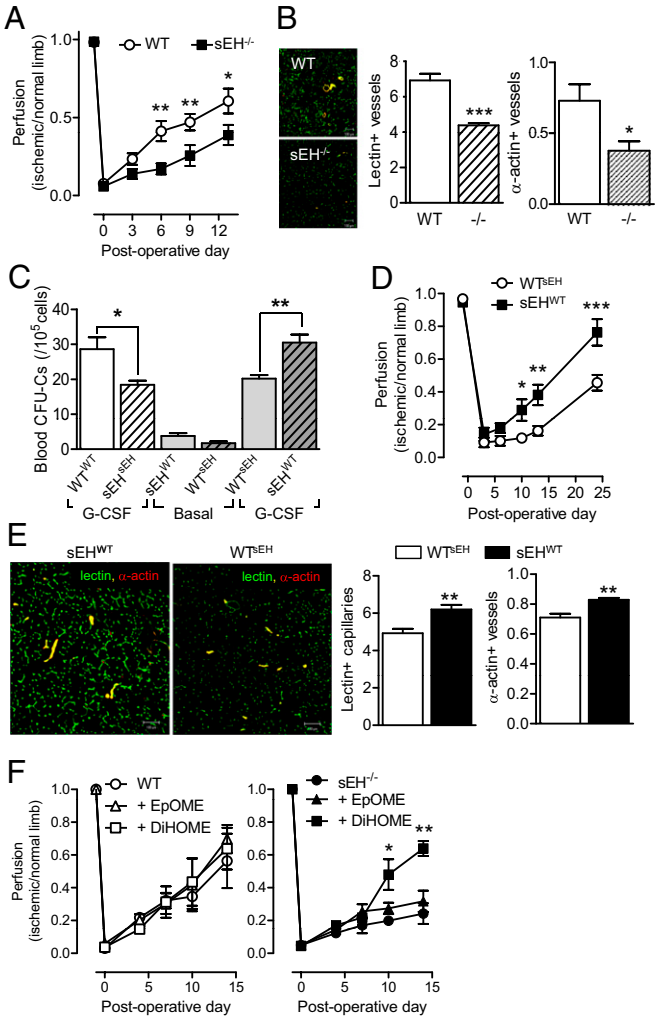

Fig. 4. Consequences of sEH deletion and bone marrow repletion on progenitor cell mobilization and vascular repair in the ischemic hindlimb. (*A*) Hindlimb perfusion in WT and sEH$^{-/-}$ mice immediately before and up to 14 d after ischemia. Perfusion was quantified as a ratio of ischemic to nonischemic limb. (*B*) Capillary and arteriole density assessed by quantification of isolectin B4 (green) and α-actin (red) staining. (*C*) CFU-C colony formation by PBMCs derived from WT and sEH$^{-/-}$ mice 16 wk after transplantation with either WT or sEH$^{-/-}$ bone marrow. Colony-forming ability was determined under basal conditions and following treatment with G-CSF (5 d). (*D*) Effect of bone marrow transplantation on the recovery of blood flow following ischemia. (*E*) Capillary and arteriole density 9 d postsurgery, quantified with isolectin B4 (green) and α-actin (red) staining. (*F*) Effect of 12,13-EpOME and 12,13-DiHOME (minipumps) on the recovery of blood flow following ischemia in WT and sEH$^{-/-}$ mice. The graphs summarize data obtained in five to six animals per group; $^*P < 0.05$, $^{**}P < 0.01$, $^{***}P < 0.001$. (Magnification: *B*, 200×; *E*, 200×.)

Discussion

The results of our study reveal a previously uncharacterized interaction between the CYP/sEH pathway and HPC proliferation, mobilization, and a subsequent role in vascularization. Loss of sEH activity resulted in a marked reduction in *cmyb*/*lmo2* double-positive cells in the zebrafish CVP and malformation of this tissue. In mice the lack of sEH expression and activity led to a diminished proliferation of short-term repopulating HPCs in the spleen, attenuated G-CSF–induced mobilization of progenitor cells, and attenuated vascular repair capacity. Mechanistically, these effects were associated with decreased β-catenin and could be rescued by supplementation with the diols 12,13-DiHOME or 11,12-DHET but not the corresponding epoxides.

Given the published reports linking EETs with increased angiogenesis, it was initially surprising to note that zebrafish lacking the sEH demonstrate an almost normal arterial vasculature but defects in the zebrafish trunk venous network; the most prominent alteration being the development of an enlarged single-channeled caudal vein and lack of the CVP. As the CVP is a complex vascular network generated from the caudal vein, these data imply that the CYP/sEH axis may be more important for venous than

arterial angiogenesis. Certainly, distinct signals are thought to dictate angiogenesis in the dorsal aorta and axial vein, with the former being dependent on VEGF-A signaling and the latter linked to bone morphogenic protein (15). Although we have no information about whether or not bone morphogenic protein signaling is affected by the deletion/inhibition of the sEH, it is important to note that EET-induced angiogenesis is dependent on the expression of the "venous marker" EphB4 (even in arterial endothelial cells). Indeed, endothelial cell sprouting and the formation of vessels in EET-containing Matrigel in vivo can be prevented by the down-regulation of EphB4 (16).

There is a clear link between the formation of the CVP and the development of the caudal hematopoietic tissue formed by the hematopoietic stem cells that emerge from the aortic endothelium and migrate to the plexus (17–19). This tissue transiently supports the expansion of blood progenitors before this function is overtaken by the thymus and kidney (20). Given the defects in the CVP related to alteration of sEH activity and expression, we focused on establishing a link between sEH activity and hematopoietic stem and progenitor cells by counting *cmyb*/*lmo2*, as well as $CD41^+$ cells. We found a reduced number of double-positive cells in the sEH morphants, as well as in normal embryos treated with a sEH inhibitor, a phenomenon associated with pronounced alterations in the epoxide/diol ratios of EET/DHET and EpOME/DiHOME. As the effects of sEH inhibition could either represent an inhibitory effect of an epoxide or the lack of a stimulatory effect of a diol, we assessed the ability of 11,12-EET/DHET and 12,13-EpOME/DiHOME to rescue *c-myb*/*lmo2*-positive cell numbers. Although 11,12-EET was without effect, 11,12-EpOME was just as effective as the sEH inhibitor in decreasing cell numbers, and both 11,12-DHET and 12,13-DiHOME were able to rescue the phenotype. This finding is the first indication that the effects of abrogating sEH activity/expression cannot simply be explained by the accumulation of one substrate (i.e., the EETs) but result from the loss of diols generated by sEH from the EETs, as well as other substrates, such as linoleic acid. At first sight, attributing a beneficial effect to 12,13-DiHOME seems to conflict with reports that it may mediate the toxicity of linoleic acid epoxides (e.g., in the acute respiratory distress syndrome) (21). However, it is important to emphasize that the latter studies addressed the effects of very high concentrations of the diol in critically ill patients. More recent studies indicate that 12,13-DiHOME inhibits rather than potentiates the respiratory burst in neutrophils (22). One additional consequence of sEH down-regulation in zebrafish was the development of a smaller eye. Exactly why eye development was affected is unclear but the sEH is expressed in the Müller glia cells that act as a pool of retinal progenitor cells and are regulated by canonical Wnt signaling/β-catenin (23).

Our next step was to transfer the observations made in zebrafish to mice. We found that the sEH was expressed in bone marrow cells, that sEH activity was substantially higher in $LinKit^+$ cells than in Lin^+ cells, and that bone marrow cells generated the EET/DHET and EpOME/DiHOME pairs detected in the zebrafish extracts. To determine the mechanism underlying the effects observed, we focused on the Wnt signaling pathway because it controls hematopoietic stem cell self-renewal in the zebrafish and mouse, as well as bone marrow repopulation (13). Neither 11,12-EET not 12,13-EpOME had any effect on β-catenin in Lin^- cells (in contrast to the zebrafish, where EpOME was just as effective as the inhibitor in decreasing the number of $cmyb^+lmo2^+$ cells). However, similar to the effects reported for prostaglandin E_2 (PGE_2) (9, 24) and lipoxygenase products (25, 26), 11,12-DHET and 12,13-DiHOME stabilized β-catenin in vitro and increased β-galactosidase activity in vivo in a reporter mouse. Both lipids also increased murine stem and short-term repopulating progenitor populations in vivo following transplantation and were able to restore spleen colony-forming ability to cells isolated from $sEH^{-/-}$ mice. In addition, the inhibition of GSK3, which targets β-catenin for degradation through the proteasome, increased progenitor cell colony formation in the spleen assay and partly reversed the effects of sEH inhibition. Such a link fits well with previous observations reporting enhanced GSK3 phosphorylation (and inhibition) in ischemic hearts from $sEH^{-/-}$ compared with WT mice after acute ischemia and reperfusion (27). PKA could also represent a point of crosstalk between lipid signaling and the Wnt pathway, as it does after PGE_2 stimulation (24). However, although the kinase can be activated by EETs (5), definitive proof of its activation by 11,12-DHET and 12,13-DiHOME is currently lacking.

In addition to the effects on progenitor cell proliferation, we found that CYP and sEH activity was acutely altered (after 48 h) when mice were treated with G-CSF. Indeed, in WT mice the levels of both EET/DHET and EpOME/DiHOME increased in bone marrow cells following the administration of the cytokine. This unexpected finding hinted that in addition to their effects on proliferation, sEH substrates/metabolites may play a potentially important role in processes involved in progenitor cell mobilization and subsequent physiological repair processes. Certainly, the G-CSF–induced mobilization of progenitor cells was attenuated in $sEH^{-/-}$ mice, as well as in WT mice treated with *t*-AUCB. Moreover the potential to influence vascularization and vascular repair was reduced, as highlighted by the fact that the number of CD31 and α-actin–positive cells recovered from SDF-1–impregnated matrices was reduced by sEH knockout. Exogenous G-CSF administration is, however, not a physiological mobilization signal, which is why we determined the ability of WT and $sEH^{-/-}$ to recover from hindlimb ischemia. This model was felt to be particularly suitable because numerous publications have documented the role of bone marrow-derived cells in this form of vascular repair (for review, see ref. 28). The recovery of blood flow was attenuated in $sEH^{-/-}$ vs. WT mice and, just as it was possible to restore *c-myb*/*lmo2* double cells in the zebrafish with 12,13-DiHOME, treating mice with this diol (but not the corresponding epoxide) accelerated the restoration of blood flow in $sEH^{-/-}$ animals to levels seen in WT mice. At first sight these data seem to contradict a report that the overexpression of CYP epoxygenases promotes angiogenesis in the ischemic rat hindlimb (29). However, it is necessary to point out that the latter studies were performed in animals with normal sEH activity and thus able to generate the PUFA diols we found to be essential for full repair in this study. Moreover, although the authors focused on generating parallels between the consequences of CYP overexpression and the in vitro actions of the EETs, no direct comparison of the biological actions of the epoxides and diols was made, and the eventual role of a bone marrow-derived cell population in the phenomena described was not addressed. It is also important to note the fact that transplantation of $sEH^{-/-}$ mice with bone marrow cells from WT animals restored bone marrow epoxide hydrolase activity in the present study; largely normalized progenitor cell mobilization and improved revascularization following hindlimb ischemia indicating that the effects observed were related to altered HPC function rather than an effect of the CYP/sEH axis on the bone marrow niche.

Taken together, our data indicate that fatty acid diols, in particular 12,13-DiHOME and 11,12-DHET, are critical modulators of progenitor cell proliferation and mobilization by activation of the canonical Wnt signaling cascade. Thus, it appears that the fatty acid diols affect hematopoietic stem cells by a mechanism similar to that of eicosanoids, such as PGE_2 and 15-hydroxyeicosatetraenoic acid (i.e., via the stabilization of β-catenin) (9, 24–26). There is currently great interest in the biology of the CYP/sEH axis because $sEH^{-/-}$ mice and sEH inhibitor-treated mice are protected against the development of some forms of hypertension and inflammation (for review, see

ref. 30). Several experimental studies have, however, provided circumstantial evidence for a role for the sEH in bone marrow cell mobilization, because although there are no obvious differences in the blood profiles of WT and sEH$^{-/-}$ animals under resting conditions, inflammation-induced tissue infiltration with potentially proangiogenic cells, such as lymphocytes, neutrophils, and macrophages, has been reduced (4, 31–34). These findings and the results of the present investigation indicate that the long-term inhibition of the sEH may prove detrimental to the resolution of infection as well as to homeostatic functions, including hematopoeitic stem cell proliferation, mobilization, and vascular repair.

Methods

Animals. C57BL/6 mice (6–8 wk old) were purchased from Charles River. sEH$^{-/-}$ mice (35) were kindly provided by Frank Gonzalez (National Institutes of Health, Bethesda, MD) and crossbred for 10 generations onto the C57BL/6 background in the animal house facility at Frankfurt University. TOP-Gal/C57Bl6 transgenic mice (14) were from the Jackson Laboratory.

Mice were housed in conditions that conform to the *Guide for the Care and Use of Laboratory Animals* published by the National Institutes of Health (NIH publication no. 85–23). All experiments were approved by the governmental authorities (Regierungspräsidium Giessen: F28/11, F28/10) and in all experiments, age-, sex-, and strain-matched animals were used. In some experiments animals were given the sEH inhibitor, *t*-AUCB (4 mg/L) in the drinking water, as previously described (36).

Transgenic *Tg(cmyb:EGFP)zf169* (9) and *Tg(lmo2:dsRed)zf73* (37) zebrafish, kindly provided by Leonard I. Zon (Children's Hospital, Boston, MA), and *Tg(kdrl-EGFP)s843* (38) were used. Embryos were raised at 28 °C in embryo buffer containing 0.003% 1-phenyl-2-thiourea to prevent pigmentation. For microscopy, embryos were anesthetized in 0.02% tricaine and mounted in 1.5% low melting-point agarose and stacks of optical sections were captured with a confocal microscope or an inverted fluorescence microscope. Projections of stacks of confocal images were generated with LSM image browser (Zeiss) and processed in Adobe Photoshop. In some studies *t*-AUCB, 14,15-EET/DHET, and 12,13-EpOME/DiHOME (all 10 μmol/L) were added to the embryo medium, as indicated in *Results*.

Statistical Analysis. Data are expressed as mean ± SEM and statistical evaluation was performed using Student *t* test for unpaired data or one-way ANOVA followed by a Bonferroni *t* test when appropriate. Values of $P < 0.05$ were considered statistically significant.

A detailed description of all of the materials, antibodies, and standard methods used appear in *SI Methods*.

ACKNOWLEDGMENTS. We thank Ingrid Kempter, Katharina Engel, and Ariane Fischer for expert technical assistance, and Christian Scherf and Eugen Kara for their help with irradiation experiments. This work was supported by the Deutsche Forschungsgemeinschaft (TR-SFB 23/A6 and Exzellenzcluster 147 "Cardio-Pulmonary Systems"); partial support was received from National Institute on Environmental Health Sciences Grant R01 ES002710. B.D.H. is a George and Judy Marcus Senior Fellow of the American Asthma Foundation.

1. Konkel A, Schunck WH (2011) Role of cytochrome P450 enzymes in the bioactivation of polyunsaturated fatty acids. *Biochim Biophys Acta* 1814:210–222.
2. Campbell WB, Gebremedhin D, Pratt PF, Harder DR (1996) Identification of epoxyeicosatrienoic acids as endothelium-derived hyperpolarizing factors. *Circ Res* 78: 415–423.
3. Fisslthaler B, et al. (1999) Cytochrome P450 2C is an EDHF synthase in coronary arteries. *Nature* 401:493–497.
4. Deng Y, et al. (2011) Endothelial CYP epoxygenase overexpression and soluble epoxide hydrolase disruption attenuate acute vascular inflammatory responses in mice. *FASEB J* 25:703–713.
5. Fleming I (2011) The cytochrome P450 pathway in angiogenesis and endothelial cell biology. *Cancer Metastasis Rev* 30:541–555.
6. Goldstone JV, et al. (2010) Identification and developmental expression of the full complement of Cytochrome P450 genes in Zebrafish. *BMC Genomics* 11:643.
7. Arand M, Cronin A, Oesch F, Mowbray SL, Jones TA (2003) The telltale structures of epoxide hydrolases. *Drug Metab Rev* 35:365–383.
8. Murayama E, et al. (2006) Tracing hematopoietic precursor migration to successive hematopoietic organs during zebrafish development. *Immunity* 25:963–975.
9. North TE, et al. (2007) Prostaglandin E_2 regulates vertebrate haematopoietic stem cell homeostasis. *Nature* 447:1007–1011.
10. Cronin A, et al. (2003) The N-terminal domain of mammalian soluble epoxide hydrolase is a phosphatase. *Proc Natl Acad Sci USA* 100:1552–1557.
11. Newman JW, Morisseau C, Harris TR, Hammock BD (2003) The soluble epoxide hydrolase encoded by EPXH2 is a bifunctional enzyme with novel lipid phosphate phosphatase activity. *Proc Natl Acad Sci USA* 100:1558–1563.
12. Hwang SH, Tsai HJ, Liu JY, Morisseau C, Hammock BD (2007) Orally bioavailable potent soluble epoxide hydrolase inhibitors. *J Med Chem* 50:3825–3840.
13. Cerdan C, Bhatia M (2010) Novel roles for Notch, Wnt and Hedgehog in hematopoesis derived from human pluripotent stem cells. *Int J Dev Biol* 54:955–963.
14. DasGupta R, Fuchs E (1999) Multiple roles for activated LEF/TCF transcription complexes during hair follicle development and differentiation. *Development* 126: 4557–4568.
15. Wiley DM, et al. (2011) Distinct signalling pathways regulate sprouting angiogenesis from the dorsal aorta and the axial vein. *Nat Cell Biol* 13:686–692.
16. Webler AC, et al. (2008) Cytochrome P450 2C9-induced angiogenesis is dependent on EphB4. *Arterioscler Thromb Vasc Biol* 28:1123–1129.
17. Chen AT, Zon LI (2009) Zebrafish blood stem cells. *J Cell Biochem* 108:35–42.
18. Kissa K, Herbomel P (2010) Blood stem cells emerge from aortic endothelium by a novel type of cell transition. *Nature* 464:112–115.
19. Bertrand JY, et al. (2010) Haematopoietic stem cells derive directly from aortic endothelium during development. *Nature* 464:108–111.
20. Burns CE, Zon LI (2006) Homing sweet homing: Odyssey of hematopoietic stem cells. *Immunity* 25:859–862.
21. Moghaddam MF, et al. (1997) Bioactivation of leukotoxins to their toxic diols by epoxide hydrolase. *Nat Med* 3:562–566.
22. Thompson DA, Hammock BD (2007) Dihydroxyoctadecamonoenoate esters inhibit the neutrophil respiratory burst. *J Biosci* 32:279–291.
23. Ramachandran R, Zhao XF, Goldman D (2011) Ascl1a/Dkk/β-catenin signaling pathway is necessary and glycogen synthase kinase-3β inhibition is sufficient for zebrafish retina regeneration. *Proc Natl Acad Sci USA* 108:15858–15863.
24. Goessling W, et al. (2009) Genetic interaction of PGE_2 and Wnt signaling regulates developmental specification of stem cells and regeneration. *Cell* 136:1136–1147.
25. Chen Y, Hu Y, Zhang H, Peng C, Li S (2009) Loss of the Alox5 gene impairs leukemia stem cells and prevents chronic myeloid leukemia. *Nat Genet* 41:783–792.
26. Kinder M, et al. (2010) Hematopoietic stem cell function requires 12/15-lipoxygenase-dependent fatty acid metabolism. *Blood* 115:5012–5022.
27. Seubert JM, et al. (2006) Role of soluble epoxide hydrolase in postischemic recovery of heart contractile function. *Circ Res* 99:442–450.
28. Tongers J, Roncalli JG, Losordo DW (2010) Role of endothelial progenitor cells during ischemia-induced vasculogenesis and collateral formation. *Microvasc Res* 79:200–206.
29. Wang Y, et al. (2005) Arachidonic acid epoxygenase metabolites stimulate endothelial cell growth and angiogenesis via mitogen-activated protein kinase and phosphatidylinositol 3-kinase/Akt signaling pathways. *J Pharmacol Exp Ther* 314: 522–532.
30. Imig JD, Hammock BD (2009) Soluble epoxide hydrolase as a therapeutic target for cardiovascular diseases. *Nat Rev Drug Discov* 8:794–805.
31. Smith KR, et al. (2005) Attenuation of tobacco smoke-induced lung inflammation by treatment with a soluble epoxide hydrolase inhibitor. *Proc Natl Acad Sci USA* 102: 2186–2191.
32. Manhiani M, et al. (2009) Soluble epoxide hydrolase gene deletion attenuates renal injury and inflammation with DOCA-salt hypertension. *Am J Physiol Renal Physiol* 297:F740–F748.
33. Zhang LN, et al. (2009) Inhibition of soluble epoxide hydrolase attenuated atherosclerosis, abdominal aortic aneurysm formation, and dyslipidemia. *Arterioscler Thromb Vasc Biol* 29:1265–1270.
34. Revermann M, et al. (2010) Soluble epoxide hydrolase deficiency attenuates neointima formation in the femoral cuff model of hyperlipidemic mice. *Arterioscler Thromb Vasc Biol* 30:909–914.
35. Sinal CJ, et al. (2000) Targeted disruption of soluble epoxide hydrolase reveals a role in blood pressure regulation. *J Biol Chem* 275:40504–40510.
36. Keserü B, et al. (2010) Hypoxia-induced pulmonary hypertension: Comparison of soluble epoxide hydrolase deletion vs. inhibition. *Cardiovasc Res* 85:232–240.
37. Zhu H, et al. (2005) Regulation of the lmo2 promoter during hematopoietic and vascular development in zebrafish. *Dev Biol* 281:256–269.
38. Jin SW, Beis D, Mitchell T, Chen JN, Stainier DY (2005) Cellular and molecular analyses of vascular tube and lumen formation in zebrafish. *Development* 132:5199–5209.